2022 IEEE International Conference on Robotics and Automation (ICRA)
May 23-27, 2022. Philadelphia, PA, USA

Telerobotically Controlled Magnetic Soft Continuum Robots for Neurovascular Interventions

Yoonho Kim[1], Emily Genevriere[1], Pablo Harker[3], Jaehun Choe[1], Marcin Balicki[2], Aman B. Patel[3], and Xuanhe Zhao[1]

***Abstract*— Despite the recent advances in continuum robots for minimally invasive surgery or interventions, their applications to endovascular neurosurgery have remained technically challenging due to the difficulty of miniaturization. Aimed at enabling robotic applications to neurovascular interventions for endovascular treatments of stroke or brain aneurysms, we present a telerobotically controlled magnetic soft continuum robot capable of active steering and navigation under externally applied magnetic fields. For magnetic steering, a seven-degree-of-freedom (7-DOF) serial manipulator is employed to place an actuating magnet that can be manipulated via real-time teleoperation of the robot arm. A motorized linear drive is used to advance or retract the magnetic soft continuum robot, the distal tip of which is steered by the actuating magnet to enable endovascular navigation in the complex cerebral vasculature. We demonstrate the system's ability to guide selective navigation in different branches of cerebral arteries using anatomical models under visual feedback. We also compare the navigational performance of our system with that of a manually controlled passive guidewire and a conventional magnet-tipped guidewire. We found that the telerobotically controlled magnetic soft continuum robot allows for safer and quicker access to hard-to-reach areas in clinically challenging anatomies by enabling smooth navigation in narrow and winding pathways.**

Keywords—vascular robotics, magnetic steering, endovascular navigation, continuum robots, telerobotic neurointervention

I. Introduction

Robotic technologies have been adopted in various areas of both open and minimally invasive surgery to enhance surgical precision and accuracy while reducing physicians' efforts and fatigue [1]. However, despite the growing needs and interest in robotically assisted interventions, their applications to endovascular treatments of neurovascular diseases such as stroke or aneurysms have remained underexplored [2]. Existing continuum robots or steerable robotic catheters based on tendon-driven actuation, which are mostly used for cardiac and peripheral vascular applications [3], are often too large in diameter to be used for neurointervention and are difficult to miniaturize down to submillimeter scales[2, 4].

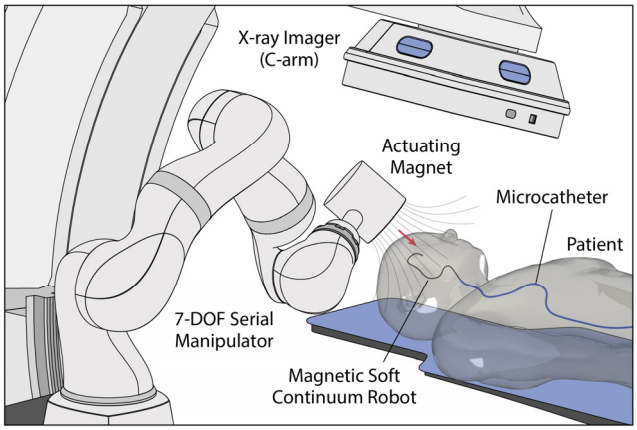

Fig. 1: Telerobotically controlled magnetic soft continuum robot in the neurovasculature based on spatial positioning of an actuating magnet at the end of a 7-DOF serial manipulator under real-time x-ray fluoroscopy.

Although some vascular robotic systems have been designed to manipulate conventional guidewires for coronary and peripheral vascular interventions [1-3, 5], they still remain unsuited for neurovascular applications due to the limited steering capabilities of such passive guidewires in narrow and tortuous intracranial arteries. Thus far, no commercial systems have been cleared for neurovascular intervention in the United States [6-9], and the feasibility of robotically assisted endovascular treatments of stroke or aneurysms in the middle or anterior cerebral arteries has not been clearly demonstrated.

For steering purposes, conventional passive guidewires have pre-shaped or shapeable distal tips that can be oriented toward a desired direction by rotating their proximal ends. However, this twist-based steering maneuver often becomes ineffective due to unpredictable and jerky motion of the prebent tip, also known as whipping, particularly when navigating in narrow and tortuous pathways under large friction [10]. To avoid risky guidewire maneuvers that can cause endothelial injury or damage such as vessel dissection or perforation, which can lead to devastating hemorrhagic complications, physicians need to verify the movement of the distal tip while manipulating the guidewire under continuous x-ray during the interventional procedures [11].

To provide active steering of intravascular devices under remote control (i.e., away from the radiation source), magnetically steerable guidewires were previously developed in the form of "magnet-tipped" design [12], with a finite-sized magnet or steel attached to the distal end of the device [13-16]. There have been some similar variants proposed, with a few small magnets embedded in the distal portion of the guidewire [17]. However, such magnet-tipped guidewires would entail

This work was supported by the National Science Foundation (EFRI-1935291) and National Institutes of Health (1R01HL153857-01) and funded in part by Philips Research through MIT-Philips research alliance.

[1] Yoonho Kim, Emily Genevriere, Jaehun Choe, and Xuanhe Zhao are with the Zhao Lab, Department of Mechanical Engineering, Massachusetts Institute of Technology, Cambridge, MA, USA. yoonho@mit.edu

[2] Marcin Balicki is with the Philips Research, Cambridge, MA, USA.

[3] Pablo Harker and Aman B. Patel are with the Department of Neurosurgery, Massachusetts General Hospital and Harvard Medical School, Boston, MA, USA. Pablo Harker is currently with the Department of Neurology and Rehabilitation Medicine, University of Cincinnati College of Medicine, Cincinnati, OH, USA.

potential risks of embolization because the magnet at the end could break off [18]. Furthermore, the use of finite-sized, rigid magnets in a thin flexible guidewire can lead to discontinuous dimensions or mechanical properties along the device, thereby compromising its compatibility with other standard interventional devices such as microcatheters for delivering therapeutic devices such as embolization coils or a stent retriever.

To tackle the existing challenges in neurointerventional procedures by enabling robotic applications to endovascular neurosurgery, we present a telerobotic neurointerventional platform that allows for remote and precise control of the magnetic soft continuum robot [4] in the complex neurovasculature. Our system is based on a 7-DOF serial robot arm manipulator with an actuating magnet at its end-effector to apply magnetic fields required for actuation and steering of the magnetic soft continuum robot (Fig. 1). The system also includes a motorized linear drive to advance or retract the magnetic soft continuum robot. In this paper, we demonstrate the steering and navigational capabilities of the telerobotically controlled magnetic soft continuum robot to enable access to different branches of cerebral arteries using realistic anatomical models, in comparison with conventional magnet-tipped guidewires as well as manually controlled passive guidewires.

II. System Description

Fig. 1 provides an overview of our system in clinical settings for image-guided neurovascular intervention based on real-time x-ray fluoroscopy to visualize the magnetic soft continuum robot navigating in the patient's neurovasculature under magnetic manipulation. The serial robot arm holding the actuating magnet is teleoperated by an operator with a joystick controller to steer the magnetic soft continuum robot by varying the position and orientation of the magnet around the patient's head. The advancing unit is also remotely controlled to advance/retract the continuum robot from its proximal end.

A. Magnetic Soft Continuum Robot

The magnetic soft continuum robot is a submillimeter-scale soft-robotic guidewire that can be controlled magnetically owing to the magnetized particles embedded in its body made of soft polymers as distributed actuation sources in the presence of externally applied magnetic fields [4, 19]. With an outer diameter of 400 μm (0.016 inches), the magnetic soft continuum robot is as thin and flexible as standard neurovascular guidewires (with outer diameters of 0.010/0.012/0.014/0.016 inches) and compatible with neurovascular microcatheters (with inner diameters of 0.017/0.021/0.027/0.033 inches).

Composed of soft polymers based on thermoplastic polyurethane (TPU) mixed with magnetizable neodymium-iron-boron (NdFeB) particles, its flexible distal tip is magnetically responsive and can be steered with an actuating magnet utilizing the magnetic torques and forces generated from the embedded magnetic dipoles under the applied fields and field gradients [19-21]. Depending on the orientation of the magnet relative to the steerable tip of the magnetic soft continuum robot, its distal tip can be either attracted toward or repelled from the actuating magnet, because of its programmed magnetic polarity that makes the distal tip behave essentially as a flexible and bendable permanent magnet. This working principle allows it to exploit different steering control modes and strategies while navigating in the complex neurovasculature.

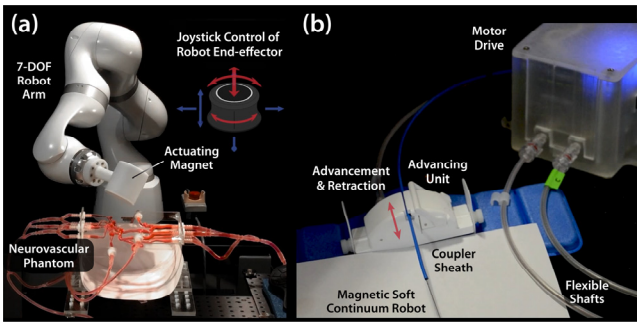

Fig. 2: (a) Steering of the magnetic soft continuum robot in the neurovascular phantom based on spatial positioning of an actuating magnet through 6-DOF pose control of the robot arm's end-effector under joystick teleoperation. (b) Advancement and retraction of the magnetic soft continuum robot through a motorized linear drive based on worm drive to convert the rotary motion of the DC motor at the base to a linear motion upon joystick control.

B. Telerobotic Magnetic Manipulation Platform

The distal tip of the magnetic soft continuum robot can be steered remotely by manipulating the actuating magnet (of cylindrical shape with diameter and thickness of 76.2 mm; axially magnetized; NdFeB) at the end-effector of the serial robot arm. While spatial positioning of the magnet in 3D space requires at most 6 DOFs, our system uses a 7-DOF serial robot arm (LBR Med 14 R820, KUKA) with 7 revolute joints, to take advantage of its kinematic redundancy for more flexible, safer operation in cluttered environments with confined workspace, as shown in Fig. 2(a). The extra DOF provides more dexterity that helps the robot arm avoid kinematic singularities and joint limits [22] as well as the workspace obstacles in clinical settings (e.g., patient, C-arm, table, and radiation shields).

The system's user interface enables spatial positioning of the actuating magnet through real-time teleoperation the robot arm's end-effector using a 6-DOF joystick controller (SpaceMouse, 3Dconnexion), with which the operator can intuitively alter the position and orientation of the magnet (Fig. 2(a)). Upon the operator's joystick control, the 6-DOF motion commands are produced as a combined set of incremental motions (translations and rotations) in each DOF, which are scaled and converted into the end-effector's linear and angular motions in the task-space coordinates. The motion commands for the end-effector are then transformed into the joint commands by multiplying the pseudo-inverse of the Jacobian, which returns the minimum-norm solution for redundant manipulators like the one used in the present study by minimizing the two-norm. The joint commands are added to the current joint positions to get new joint position values, which are sent to the robot arm controller to execute the motion that achieves the desired configuration of the robot arm.

C. Advancing Unit based on Motorized Linear Drive

The advancement or retraction of the magnetic soft continuum robot can be controlled using a motorized linear drive based on a worm gear and a drive wheel to convert the rotary motion transmitted from the DC motor at the base through a flexible shaft to a linear motion (Fig. 2(b)). The advancing unit is also remotely controlled by the operator with the joystick buttons under visual feedback from real-time x-ray imaging of the magnetic soft continuum robot in the target vasculature.

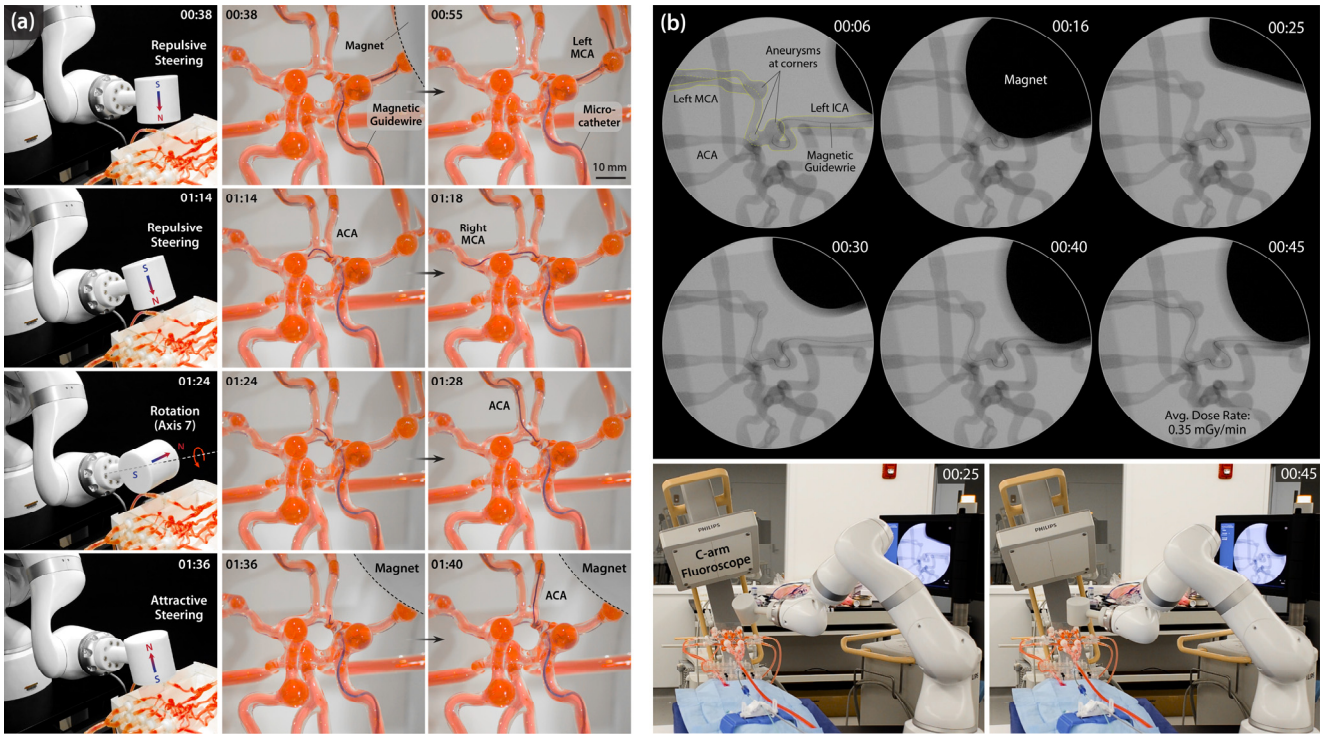

Fig. 3: Telerobotically controlled endovascular navigation in the simulated neurovasculature using the magnetic soft continuum robot. (a) Selective navigation in distal branches of the middle/anterior cerebral arteries (MCA/ACA) with the magnetic soft continuum robot through real-time teleoperation of the system under optical imaging. (b) Image-guided endovascular navigation in the left MCA of the neurovascular phantom under real-time x-ray fluoroscopy.

III. Benchtop Verification

As part of the experimental validation of our developed system, we evaluated the steering and navigational performance of the telerobotically controlled magnetic soft continuum robot using 3D-printed silicone models that replicate the human intracranial arteries (Figs. 3 and 4). These anatomical models with silicone vessels for in vitro benchtop testing were filled with a blood-mimicking fluid to simulate the friction between typical intravascular devices (e.g., guidewires/microcatheters)with hydrophilic coatings and real blood vessels.

A. Selective Navigation in Cerebral Arteries

We evaluated the steering and navigational performance of our magnetic soft continuum robot in different branches of cerebral arteries using a 3D neurovascular phantom (Trandomed 3D), as shown in Fig. 3(a). Starting from the left internal carotid artery (ICA), the magnetic soft continuum robot was first manipulated to reach the left middle cerebral artery (MCA) bifurcation, at which the magnetically steerable distal tip was directed toward the inferior branch of the MCA under repulsive steering to avoid contact with the aneurysm at the corner (MCA bifurcation) while advancing forward, as shown in Fig. 3(a) (00:38). Then, a microcatheter was advanced to travel over the guidewire along the navigated path, up to the junction between the left MCA and the anterior cerebral artery (ACA), as shown in Fig. 3(a) (00:55). After positioning the magnet such that the steerable tip of the soft continuum robot could be directed toward the left ACA under repulsive steering, the continuum robot was then advanced to reach the right MCA, across the anterior communicating artery (ACoA), as shown in Fig. 3(a) (01:14~01:18). Then, the distal tip was magnetically steered to reach the right and left distal branches of the ACA in sequence, within the ACoA complex, as shown in Fig. 3(a) (01:24~01:40).

Next, to demonstrate the compatibility of our developed system with standard image-guided procedures based on x-ray, we performed telerobotically controlled magnetic steering and navigation under real-time x-ray fluoroscopy. As shown in Fig. 3(b), the magnetic soft continuum robot was naturally visible under x-ray fluoroscopy, as clearly as standard neurovascular guidewires, due to the embedded radiopaque magnetic particles. The movement of its steerable tip in response to the actuating magnet was also clearly observed under the low dose (0.35 mGy/min) of x-ray fluoroscopy with a pulse rate of 15 p/s. To safely pass the first aneurysm at the acute-angled corner in the left ICA, the guidewire tip was directed posteriorly under repulsive steering to avoid contact with the aneurysm and then advanced up to the junction between the left MCA and the ACA, as shown in Fig. 3(b) (00:06~00:25). Then, the distal tip was oriented laterally to make a 90° turn toward the left MCA under attractive steering, to prevent it from latching onto the small aneurysm at the MCA-ACA junction, and then advanced up to the third aneurysm at the MCA bifurcation, as shown in Fig. 3(b) (00:25~00:30). The steerable tip was then directed posteriorly toward the inferior branch of the left MCA through repulsive steering and further advanced to reach the distal end of the branch without making contact with the aneurysm at the corner (MCA bifurcation), as shown in Fig. 3(b) (00:40~00:45).

These results demonstrate the capability of our telerobotically controlled soft continuum robot to selectively reach the distal branches of cerebral arteries under magnetic steering,

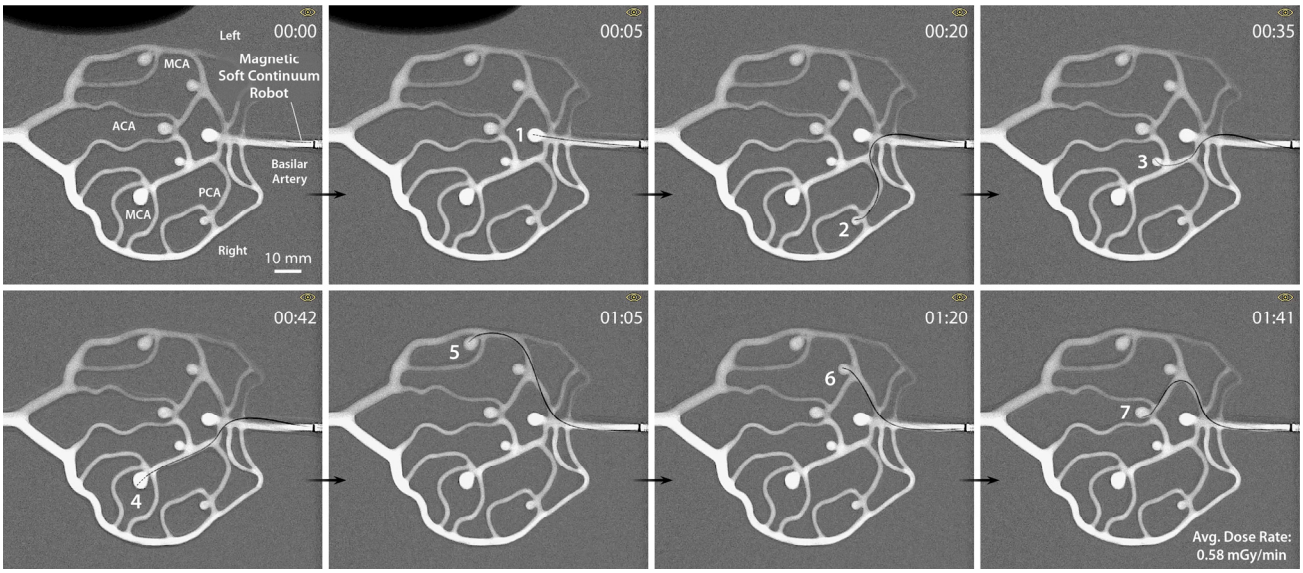

Fig.4: Magnetic soft continuum robot selectively reaching the aneurysms present in the 2D neurovascular model under real-time teleoperation of the developed system for spatial positioning of the actuating magnet relative to the steerable tip of the magnetic soft continuum robot to utilize either attractive or repulsive steering in the model vasculature under x-ray fluoroscopy.

despite the presence of complex angulation and large aneurysms at the acute-angled corners in the model cerebral vasculature. The results also illustrate that the magnetic steering and navigation in the complex cerebral vasculature can be achieved through minimal motion of the actuating magnet through real-time teleoperation of the robot arm and advancing unit from remote-control console under visual feedback.

B. Selective Access to Cerebral Aneurysms

It is worth noting that the actuating magnet did not block the view of the distal tip of the magnetic soft continuum robot during the demonstrated navigational tasks, even though it could partially show up on the optical or x-ray images (Fig. 3). To better illustrate this point regarding the steering principle for our magnetic soft continuum robot, we employed a 2D neurovascular model with planar geometry (Fig. 4). While in a simplified planar form, the model appropriately represented all native pathway attributes as well as the various anticipated curvatures and disease states such as cerebral aneurysms.

We demonstrated our system's capability to guide access to each of the aneurysms present in the model selectively through real-time teleoperation of the system under x-ray fluoroscopy (Fig. 4). Starting from the basilar artery, the magnetic soft continuum robot was first advanced to reach the first aneurysm at the basilar terminus with its straight distal tip under no effective magnetic steering as shown in Fig. 4 (00:00~ 00:05). Positioned on the left side of the 2D phantom, the actuating magnet was angled and rotated relative to the distal tip of the magnetic soft continuum robot to utilize either attractive or repulsive steering to guide its selective access to all other aneurysms in sequence, as shown in Fig. 4 (00:20~01:41). The degree of tip bending was controlled by bringing the actuating magnet either closer to or further away from the steerable tip through joystick teleoperation of the robot arm's end-effector.

As can be seen in Fig. 4, the actuating magnet did not block the view of the distal tip while it was being magnetically steered to selectively reach all the aneurysms in the model cerebral vasculature. This is because, for the 2D vascular model that was chosen on purpose to illustrate this point, the plane of view (anteroposterior projection) for state observation of the magnetic soft continuum robot corresponds to the plane on which the distal tip is being steered by the actuating magnet in the target vasculature. Hence, the magnet moving sideways (i.e., laterally to the target vasculature) should not block the view of the steerable tip of the continuum robot, even if it can partially appear on the fluoroscopic images as shown in Fig. 4. The argument that the actuating magnet would not block the view of the distal tip of the continuum robot during steering and navigation should generally hold for 3D vascular structure as well, provided that a suitable projection (i.e., the plane of view) was chosen for optimal state observation of the distal tip angle in the target vasculature.

IV. Comparison of Performance

Now that the feasibility of our proposed system for image-guided neurovascular intervention has been demonstrated from the experimental validation using anatomical models above, we compare the steering and navigational performance of our telerobotically controlled magnetic soft continuum robot with that of a manually controlled passive guidewire and a magnet-tipped guidewire, both of which were used in conventional approaches.

A. Manually Controlled Passive Guidewires

As discussed earlier, standard vascular guidewires have pre-shaped or shapeable distal tips for steering purposes based on twisting maneuver. Such conventional passive guidewires retain some functional limitations inherent in their twist-based steering especially when navigating in complex pathways with clinically challenging tortuosity due to large friction acting on the wire. To illustrate this point, we repeated the same navigational task in Fig. 3(b) using a manually manipulated 0.014-inch neurovascular guidewire with a shapeable distal tip (Synchro 2, Stryker), as presented in Fig. 5(b). The task was performed under optical imaging to avoid unnecessary x-ray exposure during the demonstration. For direct comparison,

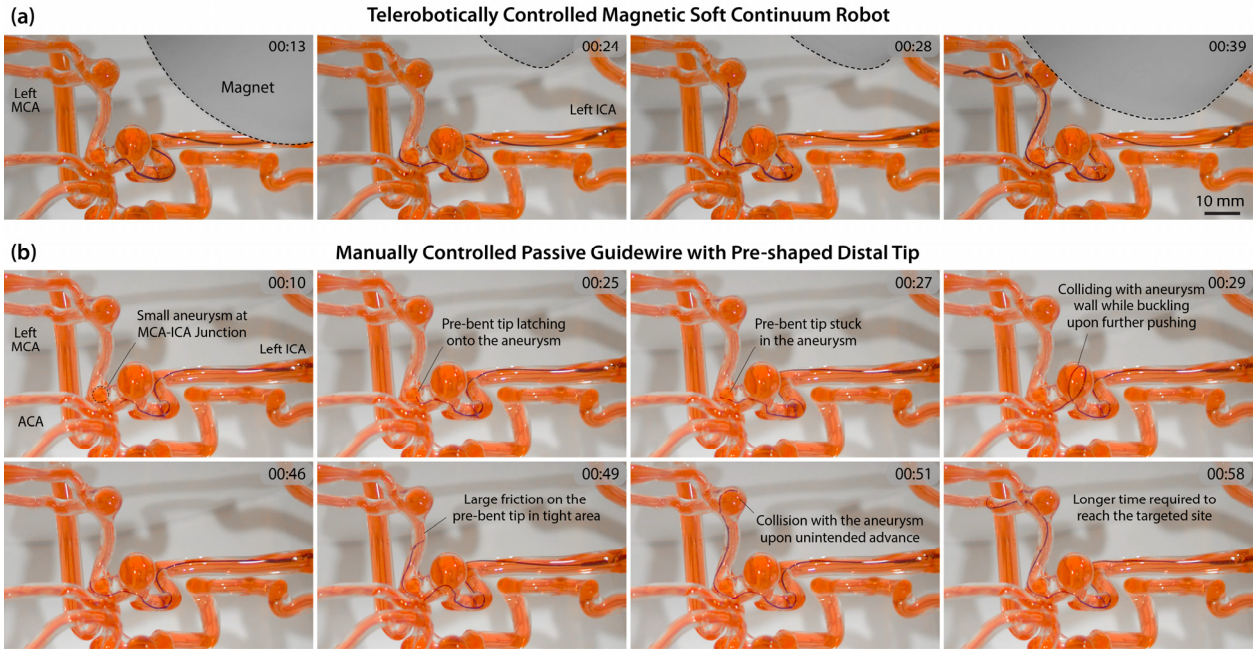

Fig.5: Evaluation of the navigational performance of the telerobotically controlled magnetic soft continuum robot in comparison with a manually controlled passive guidewire. (a) The magnetic soft continuum robot demonstrated smooth navigation in the narrow and tortuous pathways without any unexpected or unintended distal tip movements or contact with the aneurysms along the navigated path, due mainly to its active steering capability. (b) A standard neurovascular guidewire with a pre-shaped tip was used to perform the same navigational task for comparison. The pre-bent tip tended to latch onto the small aneurysm at the distal ICA or drag on the vessel wall in tight areas, causing unpredictable and undesirable motion of the guidewire such as colliding with the inner wall of the aneurysms or the vessel walls along the path. ICA: internal carotid artery, MCA: middle cerebral artery, ACA: anterior cerebral artery.

navigation of the same path using our magnetic soft continuum robot is presented in Fig. 5(a) as well.

The chosen path from the left ICA to the most distal aneurysm at the left MCA was navigated using the shapeable guidewire with a 90° tip as shown in Fig. 5(b). We noticed that the pre-bent tip tended to scrape on the vessel wall, particularly in tight and tortuous areas, causing somewhat unpredictable and abrupt movement. The pre-bent tip helped the guidewire to cross the first aneurysm present at the acutely angled carotid siphon in the left ICA as shown in Fig. 5(b) (00:10). However, upon further advancement of the proximal end without turning the guidewire, the guidewire tip was prone to fall into the posterior communicating artery (PCoA), which was unintended. When the guidewire was rotated to prevent this from happening by orienting its distal tip toward the left MCA, another undesirable situation was created as the guidewire tip latched onto the small aneurysm located at the distal end of the ICA, which led to unstable, risky behavior such as colliding with the vessel wall while buckling or looping in the first aneurysm in the left ICA, as can be seen in Fig. 5(b) (00:25~00:29). The distal tip scraping onto the vessel wall was also observed in the left MCA, which led to collision of the guidewire tip with the third aneurysm at the MCA bifurcation upon sudden release of the tension built up in the guidewire due to friction and subsequent unintended movement of the guidewire, as shown in Fig. 5(b) (00:49~00:51).

On the contrary, the active steering capability of our magnetic soft continuum robot to deflect its distal tip on demand obviated such unexpected or unintended tip movements, as demonstrated in Figs. 3(b) and 5(a), and helped to reduce the procedural time and the potential risk of complications due to vessel perforation or aneurysm rupture. Overall, the time it took for the distal tip to reach the targeted area (inferior branch of left MCA) was longer with the manually controlled passive guidewire (65 s) than with the telerobotically controlled magnetic soft continuum robot (40 s). Given the limited steerability of manually controlled passive guidewires due to unpredictable behavior, we believe that the demonstrated steering and navigational capabilities of our telerobotically controlled magnetic soft continuum robot suggests potential for advancing endovascular neurosurgery by enabling safer and quicker access to hard-to-reach areas while minimizing the radiation exposure to interventionalists.

B. Conventional Magnet-tipped Guidewires

Lastly, we compared the steering and navigational performance of our magnetic soft continuum robot with that of the conventional magnet-tipped design based on a rigid, finite-sized magnet attached to the distal end of a flexible guidewire. The magnet-tipped guidewire for comparison was fabricated by attaching a cylindrical NdFeB magnet (axially magnetized) with diameter of 400 μm and length of 4 mm at the distal end of a 0.016-inch neurovascular guidewire (Headliner, Terumo). The potted magnet was coated with a thin layer of soft composite based on TPU mixed with tungsten powder, where the tungsten particles were used as nonmagnetic radiopaque fillers. For fair comparison, other mechanical properties and dimension of the magnet-tipped guidewire were designed to be close to those of our magnetic soft continuum robot except for the distal portion with the embedded rigid magnet. The outer diameter of the distal tip of the magnet-tipped guidewire was approximately 600 μm, due to the presence of the finite-sized magnet within the polymer jacket, and further miniaturization

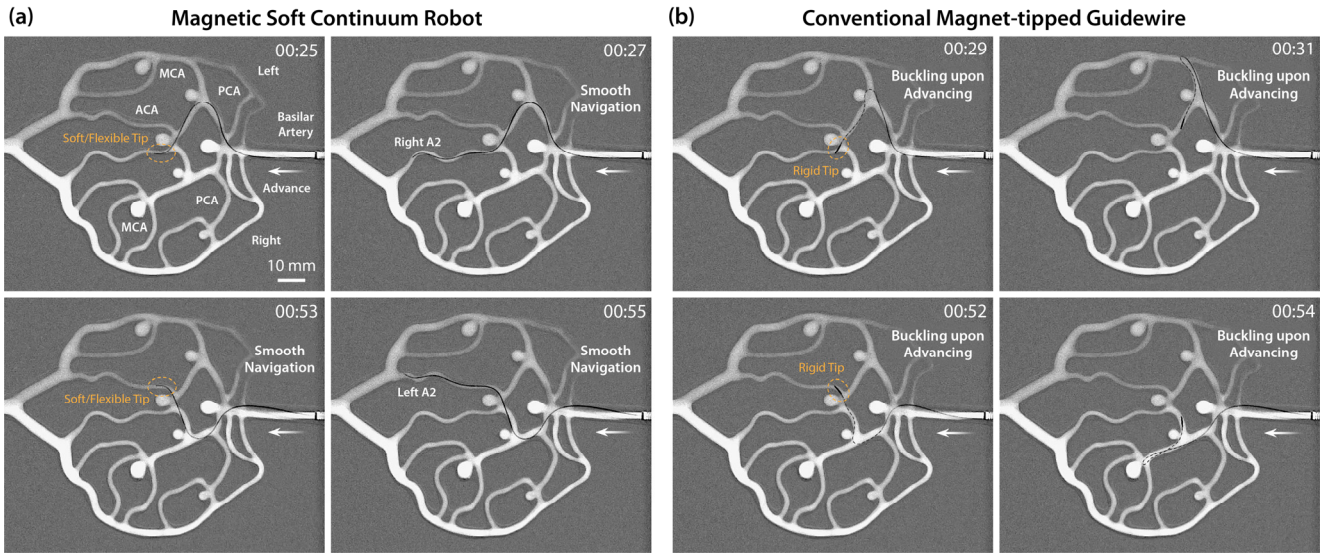

Fig. 6: Comparison of navigational performances of (a) the magnetic soft continuum robot with its soft and flexible distal tip and (b) the conventional magnet-tipped guidewire with its rigid and stiff distal tip. The flexible distal tip of the magnetic soft continuum robot enables smooth navigation in the tight and tortuous areas in the ACA, whereas the rigid and stiff tip of the magnet-tipped guidewire prevents it from working through the target vasculature due to the lack of ability to conform to the given environment, which leads to the buckling and herniation of the guidewire in the middle of the navigated path upon further advancement. ACA: anterior cerebral artery, MCA: middle cerebral artery, PCA: posterior cerebral artery.

was practically infeasible because the potted NdFeB magnet was prone to brittle fracture during the fabrication process when even thinner magnets were used to reduce the diameter.

We hypothesized that the rigid and stiff distal tip of the magnet-tipped guidewire could make it difficult to work through narrow and winding pathways in the distal cerebral vasculature as it lacks the ability to conform to the given environment. To validate this, we chose to navigate the distal branches of cerebral arteries in the 2D neurovascular model using our magnetic soft continuum robot and the magnet-tipped guidewire. For fair comparison of their navigational performances, both were manipulated using our telerobotic neurointerventional platform.

As demonstrated in Fig. 6(b), the magnet-tipped guidewire tended to buckle in the middle of the navigated path upon further advancement and herniate into the open space of an undesired branch, as the rigid distal tip did not allow the guidewire to pass the sharp corners in the tight areas of the ACA. This undesirable event was repeatedly observed in other similarly narrow and winding pathways in the model neurovasculature, validating the above-mentioned hypothesis. On the contrary, our magnetic soft continuum robot demonstrated the ability to conform to the environment using its soft and flexible distal tip and smoothly navigated the narrow and winding pathways of the model cerebral vasculature, as can be seen in Fig. 6(a). This result illustrates the unique advantage of our magnetic soft continuum design over the conventional magnet-tipped guidewires in realizing structurally simple yet effective means of magnetic steering at submillimeter scales for neurovascular applications.

V. Conclusions and Future Work

Through the series of benchtop testing with in vitro phantom models, we have demonstrated the feasibility of our proposed system for robotically assisted neurovascular intervention based on the magnetically steerable soft continuum robot and the telerobotic manipulation system for remote control of the magnetic soft continuum robot. We have also demonstrated that our system's capability to guide smoother, safer, and faster endovascular navigation in the complex neurovasculature, when compared with both manual and magnet-tipped guidewires. In future studies, we will further investigate the applicability of our system in actual clinical settings for endovascular treatments of stroke and brain aneurysms, with more realistic workspace constraints due to patient geometry and nearby objects taken into account. This will include, for example, identifying the optimal size and shape of the actuating magnet for use in actual clinical settings. In addition, animal testing will be required to further validate the safety and effectiveness of the magnetic soft continuum robot by evaluating its steering and navigational performance under realistic in vivo conditions with the viscoelastic and physiological responses of real blood vessels considered.

References

[1] J. Troccaz, G. Dagnino, and G.-Z. Yang, "Frontiers of medical robotics: from concept to systems to clinical translation," *Annu. Rev. Biomed. Eng.*, vol. 21, no. 1, pp. 193-218, 2019.

[2] S. A. Menaker, S. S. Shah, B. M. Snelling, S. Sur, R. M. Starke, and E. C. Peterson, "Current applications and future perspectives of robotics in cerebrovascular and endovascular neurosurgery," *J. Neurointerv. Surg.*, vol. 10, no. 1, pp. 78-82, 2018.

[3] J. Bonatti, G. Vetrovec, C. Riga, O. Wazni, and P. Stadler, "Robotic technology in cardiovascular medicine," *Nat. Rev. Cardiol.*, vol. 11, no. 5, pp. 266-275, 2014.

[4] Y. Kim, G. A. Parada, S. Liu, and X. Zhao, "Ferromagnetic soft continuum robots," *Sci. Robot.*, vol. 4, no. 33, eaax7329, 2019.

[5] J. Chakravartti and S. V. Rao, "Robotic assisted percutaneous coronary intervention: hype or hope?," *J. Am. Heart Assoc.*, vol. 8, no. 13, 2019.

[6] V. M. Pereira et al., "First-in-human, robotic-assisted neuroendovascular intervention," *J. Neurointerv. Surg.*, vol. 12, no. 4, pp. 338-340, 2020.

[7] G. W. Britz, J. Tomas, and A. Lumsden, "Feasibility of robotic-assisted neurovascular interventions: initial experience in flow model and porcine model," *Neurosurgery*, vol. 86, no. 2, pp. 309-314, 2019.

[8] K. C. Sajja et al., "Endovascular robotic: feasibility and proof of principle for diagnostic cerebral angiography and carotid artery stenting," *J. Neurointerv. Surg.*, vol. 12, no. 4, pp. 345-349, 2020.

[9] V. M. Pereira *et al.*, "Feasibility of robot-assisted neuroendovascular procedures," *J. Neurosurg.,* pp. 1-13, 2021. doi: 10.3171/2021.1.Jns2036
17.

[10] U.S. Food and Drug Administration (FDA), Center for Devices and Radio-logical Health. FDA-2018-D-1775, *Coronary, Peripheral, and Neuro-vascular Guidewires – Performance Tests and Recommended Labeling*.

[11] C. E. Hoffler and A. M. Ilyas, "Fluoroscopic radiation exposure: are we protecting ourselves adequately?," *J. Bone Jt. Surg*., vol. 97, no. 9, pp. 721-725, 2015.

[12] Y. Kim and X. Zhao, "Magnetic Soft Materials and Robots, " *Chem. Rev.*, 2022/02/01 2022, doi: 10.1021/acs.chemrev.1c00481.

[13] T. Krings et al., "Magnetic versus manual guidewire manipulation in neuroradiology: in vitro results," *Neuroradiology*, vol. 48, no. 6, pp. 394-401, 2006.

[14] M. Schiemann, R. Killmann, M. Kleen, N. Abolmaali, J. Finney, and T. J. Vogl, "Vascular guide wire navigation with a magnetic guidance system: experimental results in a phantom," *Radiology*, vol. 232, no. 2, pp. 475-481, 2004.

[15] K. Tsuchida et al., "Guidewire navigation in coronary artery stenoses using a novel magnetic navigation system: first clinical experience," *Catheter. Cardiovasc. Interv.*, vol. 67, no. 3, pp. 356-363, 2006.

[16] S. Ramcharitar, M. S. Patterson, R. J. van Geuns, C. van Meighem, and P. W. Serruys, "Technology insight: magnetic navigation in coronary interventions," *Nat. Clin. Pract.*, vol. 5, no. 3, pp. 148-156, 2008.

[17] S. Jeon et al., "A magnetically controlled soft microrobot steering a guidewire in a three-dimensional phantom vascular network," *Soft Robot*., vol. 6, no. 1, pp. 54-68, 2018.

[18] U.S. Food and Drug Administration (FDA). 510(K) Number: K021363, FDA, *Class 2 Medical Device Recalls: Cronus Endovascular Guidewires*.

[19] L. Wang, Y. Kim, C. F. Guo, and X. Zhao, "Hard-magnetic elastica," *J. Mech. Phys. Solids*, vol. 142, p. 104045, 2020.

[20] Y. Kim, H. Yuk, R. Zhao, S. A. Chester, and X. Zhao, "Printing ferromagnetic domains for untethered fast-transforming soft materials," *Nature*, vol. 558, no. 7709, pp. 274-279, 2018.

[21] R. Zhao, Y. Kim, S. A. Chester, P. Sharma, and X. Zhao, "Mechanics of hard-magnetic soft materials," *J. Mech. Phys. Solids*, vol. 124, pp. 244-263, 2019.

[22] S. Chiaverini, G. Oriolo, and I. D. Walker, "Kinematically redundant manipulators," in *Springer Handbook of Robotics*, B. Siciliano and O. Khatib Eds.: Springer Nature, 2008, pp. 245-268